Electronic Supporting Information for:

A Hydrothermally Stable Ytterbium Metal-Organic Framework as a Solid-Acid Catalyst for Glucose Conversion

S1: Materials Synthesis

*S1.1 Synthesis of $Yb_2(BDC)_3(DMF)_2(H_2O)_2$ **(1)***

The method described in our previous work[1] was used: ytterbium(III) chloride hexahydrate (1 mmol) and nenzene-1,4-dicarboxylic acid (1.5 mmol) were combined with stirring with 2.5 mL deionised water and 2.5 mL *N*,*N*-dimethylformamide (DMF). The mixture was sealed in a 20 mL Teflon-lined steel autoclave and heated at 100 °C for 20 hours. The resulting material was collected via vacuum filtration, washed in DMF by stirring at room temperature overnight, collected via centrifugation and rewashed in ethanol, collected again and dried at 70 °C overnight in air. Powder XRD confirmed the identity of the solid product.

*S1.2 Synthesis of $Yb_6(BDC)_7(OH)_4(H_2O)_4{\cdot}2(H_2O)$ **(2)** from **(1)***

This compound was prepared by mixing 0.2g of finely ground **(1)** and 0.1g of ytterbium chloride hexahydrate (Sigma Aldrich) in 10 ml of water. The suspension was stirred for 5 minutes before being sealed in a 20 ml Teflon lined stainless steel autoclave and heated at 200°C for 72 hours. The resulting material was collected via vacuum filtration, washed in DMF by stirring at room temperature overnight, collected via centrifugation and rewashed in ethanol, collected again and dried at 70 °C overnight in air.

*S1.3 Synthesis of **(3)***

A method based on that of Weng *et al.*[2] was used to attempt to prepared **(2)** directly, instead forming a phase-pure sample of **(3)**. A solution was prepared containing 0.08 g ytterbium nitrate hexahydrate (Sigma Aldrich) and 0.02 g sodium acetate trihydrate (Fisher Scientific) in 10 ml of water. Sodium hydroxide 0.5 M was added dropwise to the solution to yield a solution of pH 5 (typically 2 drops) and the resulting solution was then stirred for 5 minutes prior to the addition of 0.017 g of benzene-1,4-dicarboxylic acid. The mixture was then stirred for a further 5 minutes before being sealed in a 25 ml Teflon lined stainless steel autoclave at 200 °C for 72 hours. The resulting solid material was then collected via vacuum filtration, washed in DMF overnight to remove excess benzene-1,4-dicarboxylic acid, collected *via* centrifugation and rewashed in ethanol, collected again and dried at 70 °C overnight.

*S1.4 Synthesis of **(4)***

$YbCl_3{\cdot}6H_2O$ (1 mmol) and monosodium 2-sulfo-benzene-1,4-dicarboxylate acid (TCI Chemicals). (1.5 mmol) were dissolved with stirred into a DMF (5 ml) and H_2O (0.15 mL) mixture for 10 minutes. The mixture was transferred to a Teflon-lined autoclave (45 mL) and heated under solvothermal condition at 373 K for 20 hours. After cooling to room temperature, the solid product was isolated by suction filtration and washed with DMF before being dried overnight at 60 °C in air.

S2. Materials Characterisation

S2.1 Powder XRD

Preliminary sample identification was performed using a Siemens D5000 diffractometer equipment with Cu Kα1/2 radiation with data recorded in Bragg-Brentano mode. For profile fitting to confirm sample identity, data were recorded either using a a Panalytical X'Pert Pro MPD equipped with a curved Ge Johansson monochromator, giving pure Cu $K_{\alpha 1}$ radiation and a solid state PiXcel detector, where the powder was mounted on a zero-background offcut-Si holder, spinning at 30 rpm with a step size of 0.013 °, or on I11 of the Diamond Light Source from samples contained in thin-walled quartz capillaries with an X-ray wavelength of 0.825008 Å. Full pattern fitting by the Pawley method was used to refined lattice parameters using the software GSAS.[3] Table S1 contains refined lattice parameters for materials, compared with those determined by single crystal diffraction (see following section).

Table S1: Refined unit cell parameters for (2) studied by powder X-ray diffraction (room temperature, space group $P\bar{1}$)

	a / Å	*b* / Å	*c* / Å	*α* / °	*β* / °	*γ* / °
Single crystal	11.34946(16)	11.97590(19)	12.97316(18)	86.754(1)	67.0670(1)	72.156(1)
Powder XRD	11.35676(16)	11.9835(2)	12.98603(17)	86.719(2)	67.079(1)	72.130(1)
Powder XRD post catalysis	11.2622(7)	11.8887(8)	12.9074(11)	86.654(5)	67.034(5)	72.221(4)

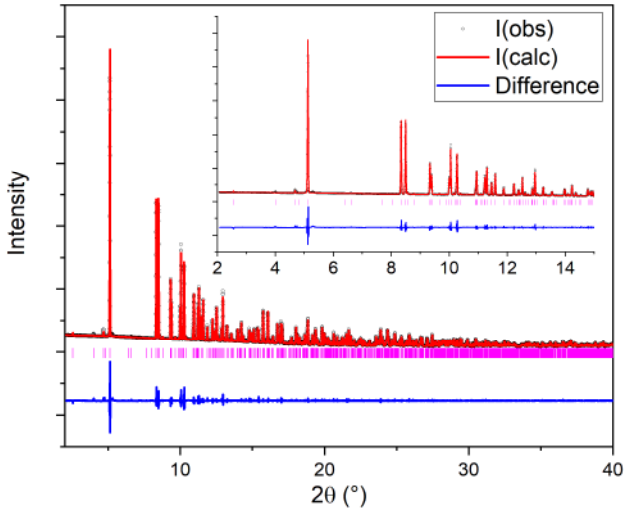

a/Å	*b*/Å	*c*/Å	*β*/°	*V*/Å³
21.56947 (8)	5.235238 (17)	22.20050 (9)	114.760 (1)	2276.444 (15)

Figure S1: Powder XRD Le Bail fit (*P*21/*n*) of a bulk sample of $Yb_2(BDC)_3$ (3) using the single crystal structure model as a starting point (λ = 0.825008 Å). The data points are black triangles, the fitted pattern the red line, the difference curve the grey line and the blue ticks the positions of allowed Bragg peaks.

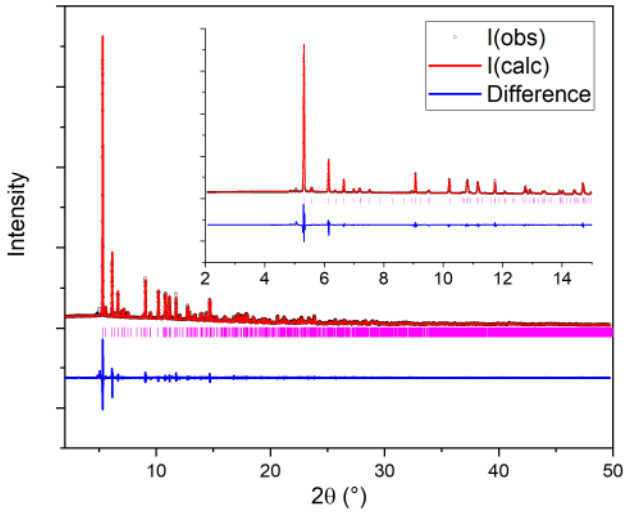

a/Å	*b*/Å	*c*/Å	*V*/Å^3
15.36810 (11)	14.19143 (11)	16.9404 (2)	3694.64 (6)

Figure S2: Powder XRD Le Bail fit (*Pbca*) of a bulk sample of [Yb(MSBDC)(DMF)$_2$] (4) using the single crystal structure model as a starting point (λ = 0.825008 Å). The data points are black triangles, the fitted pattern the red line, the difference curve the grey line and the blue ticks the positions of allowed Bragg peaks.

S2.2 Single-crystal XRD

For **(2)** and **(4)** suitable crystals were selected and mounted on glass fibres with silicon grease and placed on a Rigaku Oxford Diffraction SuperNova diffractometer with a dual source (Cu at zero) equipped with an AtlasS2 CCD area detector. The crystals were kept at 293(2) K during data collection.

For **(3)** a suitable crystal was selected and mounted on a glass fibre with Fromblin oil and placed on an Xcalibur Gemini diffractometer with a Ruby CCD area detector. The crystal was kept at 150(2) K during data collection.

Using Olex2[4] the structures were solved with the ShelXT[5] structure solution program using Intrinsic Phasing and refined with the ShelXL[6] refinement package using Least Squares minimisation.

Table S2: Selected single crystal data for the materials studied

Compound	**(2)**	**(3)**	**(4)**
CCDC reference	1892237	1892235	1892236
Empirical formula	$C_{28}H_{22}O_{19}Yb_3$	$C_{24}H_{12}O_{12}Yb_2$	$C_{14}H_{17}N_2O_9SYb$
Formula weight / gmol^{-1}	1181.57	838.42	562.39
Temperature /K	293(2)	150(2)	293(2)
Crystal system	triclinic	monoclinic	orthorhombic
Space group	$P\bar{1}$	$P2_1/n$	*Pbca*
a /Å	11.34947(16)	21.5182(7)	15.35690(19)
b /Å	11.97590(19)	5.23670(10)	14.18712(18)
c /Å	12.97316(18)	22.1791(7)	16.9515(2)
α /°	86.7541(12)	90	90
β /°	67.0669(13)	115.096(4)	90
γ /°	72.1561(13)	90	90
Volume /Å^3	1541.85(4)	2263.30(13)	3693.22(8)
Z	2	4	8
ρ_{calc}g/cm^3	2.545	2.461	2.023
M /mm^{-1}	9.113	8.284	5.228
F(000)	1104.0	1568.0	2184.0
Crystal size /mm^3	0.1 × 0.08 × 0.04	0.2 × 0.1 × 0.08	0.1 × 0.08 × 0.02
Radiation (λ / Å)	MoKα (λ = 0.71073)	MoKα (λ = 0.71073)	MoKα (λ = 0.71073)
2Θ range for data collection/°	5.126 to 61.28	5.532 to 59.856	6.196 to 65.55
Index ranges	−15 ≤ h ≤ 16, -17 ≤ k ≤ 17, -18 ≤ l ≤ 18	−30 ≤ h ≤ 29, -7 ≤ k ≤ 7, -30 ≤ l ≤ 30	−22 ≤ h ≤ 22, -21 ≤ k ≤ 20, -25 ≤ l ≤ 23
Reflections collected	51354	18097	54685
Independent reflections	8766 [R_{int} = 0.0350, R_{sigma} = 0.0237]	18097 [R_{int} = n/a, R_{sigma} = 0.0292]	6447 [R_{int} = 0.0361, R_{sigma} = 0.0226]
Data/restraints/parameters	8766/5/462	18097/0/344	6447/24/248
Goodness-of-fit on F^2	1.067	1.048	1.139
Final R indexes [I>=2σ (I)]	R1 = 0.0173, wR2 = 0.0377	R1 = 0.0421, wR2 = 0.1145	R1 = 0.0290, wR2 = 0.0581
Final R indexes [all data]	R1 = 0.0202, wR2 = 0.0387	R1 = 0.0475, wR2 = 0.1170	R1 = 0.0406, wR2 = 0.0618
Largest diff. peak/hole / e Å^{-3}	1.63/−0.75	2.63/−1.99	1.30/−0.95

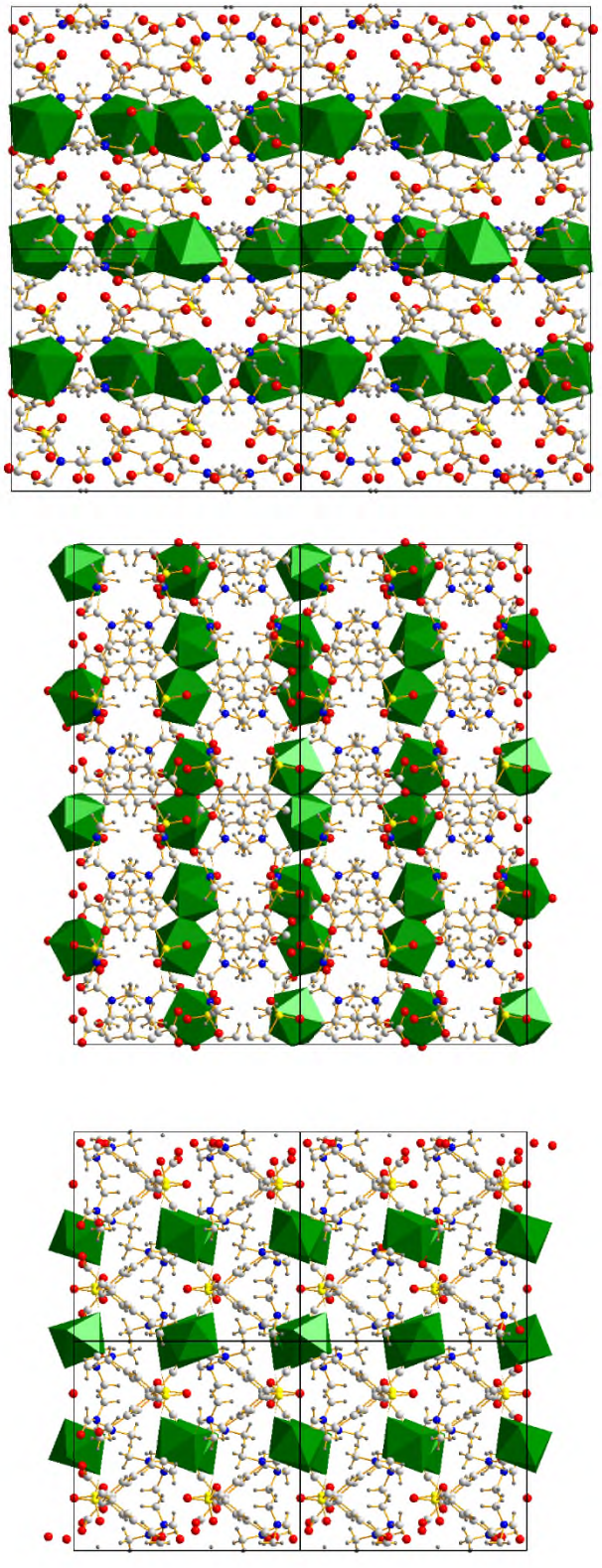

Figure S2: Overall views of the crystal structure of (4), along *a* (top), *b* (middle) and *c* (bottom), with 7-coordinated Yb centres shown as green polyhedral. Oxygen are shown as olive spheres, oxygen red, sulfur yellow, carbon light grey, nitrogen blue and hydrogen dark grey.

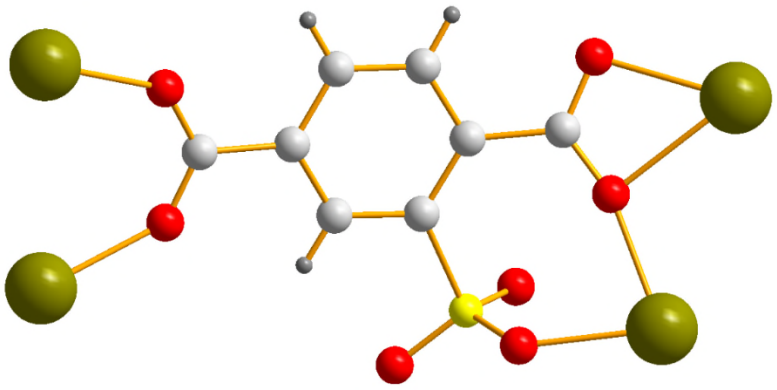

Figure S2: The local environment and connectivity of Yb centres in (4) showing the coordination of the sulfo group directly to Yb. Yb are shown as olive spheres, oxygen red, sulfur yellow, carbon light grey and hydrogen dark grey.

S2.3 Thermogravimetry/differential scanning calorimetry (TGA/DSC)

The stability of the materials, and confirmation of their composition was studied by thermogravimetric analysis (TGA) using a Mettler Toledo TGA/DSC1 instrument under ambient air pressure and a heating rate of 10 °C ·min^{-1}. Samples were heated in air from 25 °C to 1000 °C.

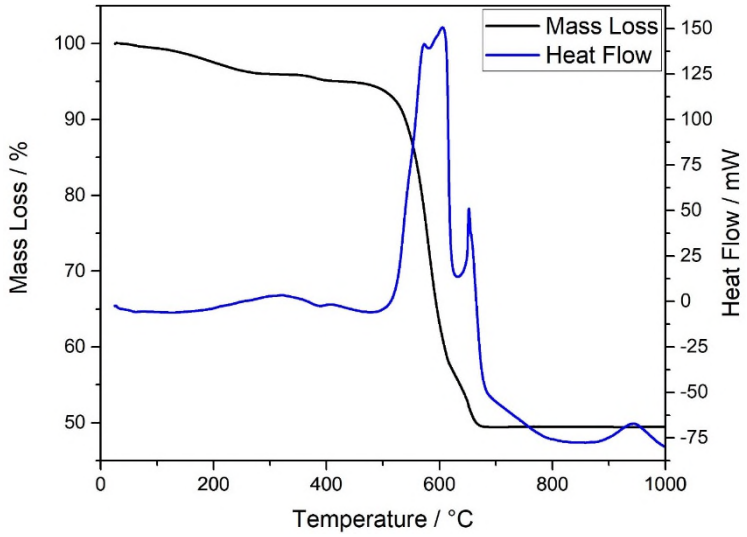

Figure S4: TGA-DSC trace of $Yb_6(BDC)_7(OH)_4(H_2O)_4 \cdot 2(H_2O)$ (2), showing initial loss of all crystal water to 300 °C (observed mass loss = 4.2 %, expected 4.6 %) and complete combustion to Yb_2O_3 (observed total mass loss = 50.6 %, expected 49.9 %).

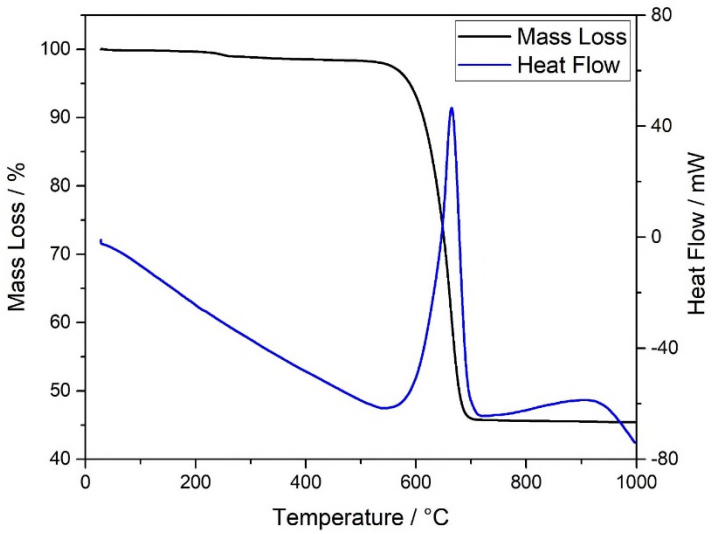

Figure S5: TGA-DSC trace of $Yb_2(BDC)_3$ (3), showing combustion of organic to give Yb_2O_3 (observed total mass loss = 54.6 %, expected 52.3 %).

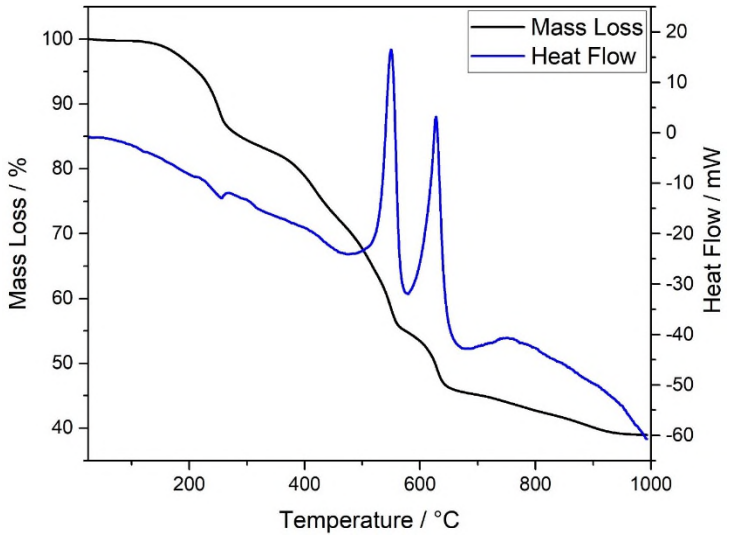

Figure S6: TGA-DSC trace of $Yb(MSBDC)(DMF)_2$ (4), showing combustion of organic to give Yb_2O_3 (observed total mass loss = 61.0 %, expected 65.0 %).

S2.4 Activation of (2)

Nitrogen adsorption measurements were made using a Micromeritics ASAP2020 apparatus, with the sample pre-treated under vacuum at 200 °C for 8 hours to remove water. This experiment showed no nitrogen accessible porosity, and a single point surface area at P/P_0 = 0.092231288 was measured as 4.79 m²/g.

Since the TGA (see above) showed loss of water at ~200 °C, *in situ* X-ray thermodiffractometry was used to check that the sample showed no collapse on heating, Figure S7 (Bruker D8 diffractometer fitted with an Anton-Parr HTK900 heating stage and operated in flowing air). This shows that on heating to 300 °C, above the loss of all crystal water, crystallinity is maintained, albeit with some adjustment of the crystal structure evident. Upon cooling to room temperature in air the initial pattern is recovered, consistent with re-adsorption of water. These results shows that **(2)** possesses zeolitic water, but the porosity does not allow nitrogen uptake and hence it is unlikely that glucose is adsorbed into the framework, implying that the catalytic activity is due to the surface of the material.

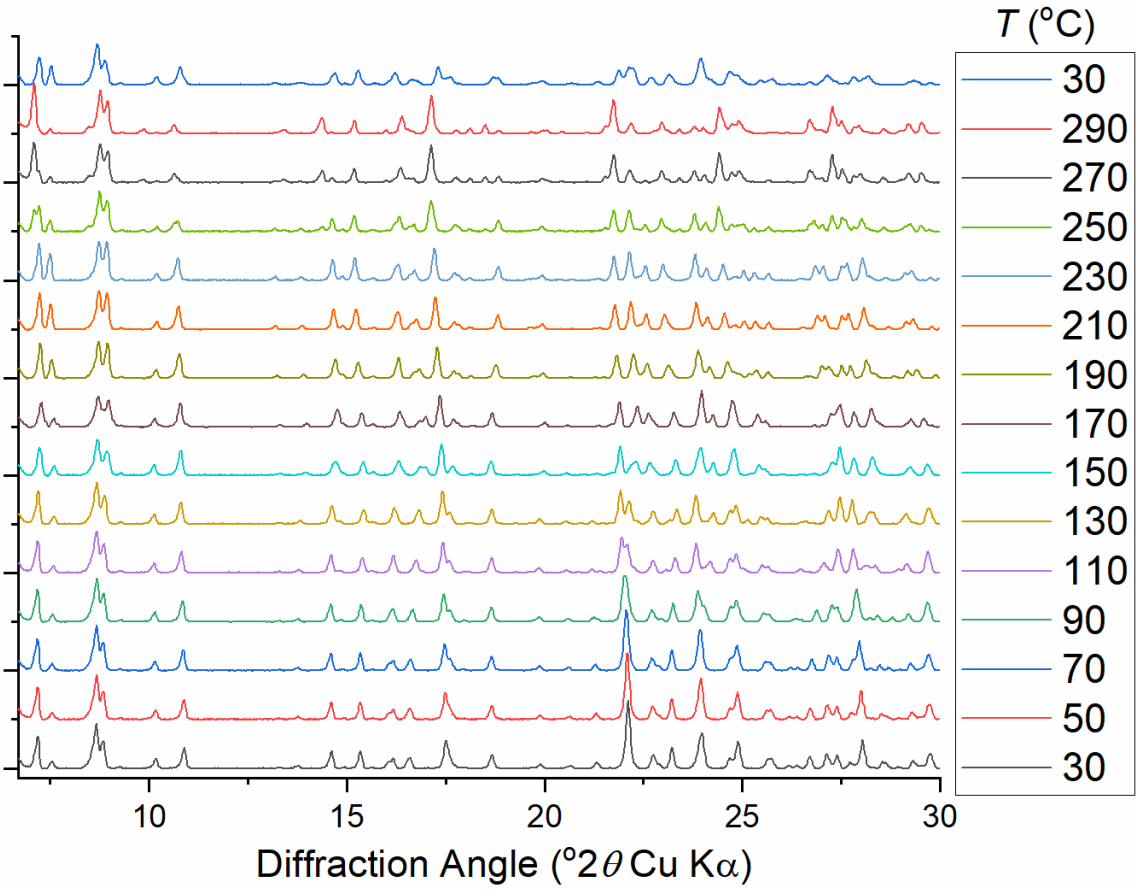

Figure S7: *In situ* X-ray thermodiffractometry on heating of (2) in air (bottom to top)

S2.5 Catalysis Testing

Catalytic screening was carried out in 5 mL batch reactors at 140 °C. 3 mL of 10 % of glucose solution (in water) was heated to the desired temperature together with 10 mg g of the catalyst for 3 hours. Each solid was heated at 200 °C for 2 hours in air before use. Blank experiments were also carried out without catalyst, and a solution of $YbCl_3$ was studied for comparison. The products were analysed by high performance liquid chromatography (HPLC) equipped with a Bio-Rad HPX 87H column; a photo diode array (PDA, at λ = 190-380 nm) detector and evaporative light scattering detector (ELSD) were used to monitor 5-HMF and sugars, respectively. The mobile phase was 0.005 M H_2SO_4 with 0.6 mL min-1 flow rate. The products fructose, mannose and 5-HMF, and the reactant (glucose) were quantified by calibration with external standard solutions.

Recycle reactions were conducted in a 25 mL reactor with PTFE lining (Berghof, BR-25). In a typical reaction, 200 mg of catalyst and a magnetic stirring bar was placed into the reactor. 15 mL of a solution of 10 wt. % glucose in water was then added. The reactor was sealed and pressurised to 10 bar with helium to ensure consistent conditions were always applied. The reactor was brought to reaction temperature (140 °C) by placing it into a preheated aluminium block heated via an IKA heating/stirring plate. At the end of the reaction (24 hours), the reactor was removed from the heating block and quenched in an ice bath at 0 °C to stop the reaction. The reactor was then depressurised and opened. The solid catalyst was recovered from the reaction solution using a centrifuge and washed with DMSO. The reaction solution was filtered and analysed using a Shimadzu HPLC as described above. In the subsequent reaction tests, the recovered catalyst was added back into the 25 mL reactor along with fresh stock solution. The reaction procedure was then repeated under the same conditions in order the test the recyclability of the catalyst and products were analysed as described above.

Table S3: Summary of catalysis results from reactions performed at 140 °C. Product selectivity is defined as 100 × (product yield/conversion), while the total desired product selectivity is the selectivity towards fructose + mannose + 5-HMF. Data are plotted in Figure 3 of the main paper.

Catalyst	pH	Time / hours	Glucose Conversion (%)	Product yield (% mole)			Product selectivity (% mole)			Total desired product selectivity (% mole)
				Fructose	Mannose	5-HMF	Fructose	Mannose	5-HMF	
None	7	3	5.6	0.8	0.0	2.1	14.3	0.0	37.5	51.8
$YbCl_3$ (*aq*)	7	3	32.1	4.6	0.3	10.6	14.3	0.9	33.0	48.3
Yb_2O_3	7	3	9.5	1.4	0.0	0.1	14.7	0.0	1.1	15.8
(2)	7	1.5	8.9	3.3	0.1	1.4	37.1	1.1	15.7	53.9
(2)	7	3	14.9	5.0	0.2	3.2	33.6	1.3	21.5	56.4
(2)	7	6	24.3	6.5	0.2	7.3	26.7	0.8	30.0	57.6
(2)	7	24	27.6	1.2	0.0	17.8	4.3	0.0	64.5	68.8
(2)	2.5	1.5	9.8	2.8	0.0	1.4	28.6	0.0	14.3	42.9
(2)	2.5	3	15.6	4.2	0.0	3.6	26.9	0.0	23.1	50.0
(2)	2.5	6	24.7	5.1	0.1	7.6	20.6	0.4	30.8	51.8
(2)	2.5	24	45.6	1.5	0.2	18.8	3.3	0.4	41.2	45.0

Table S3: Summary of recyclability catalysis results for (2) from reactions performed at 140 °C at pH = 7 for 24 hours. Data are plotted in Figure 4 of the main paper. Note that these were performed at larger scale than the data in Table S2.

Run	Glucose Conversion (%)	Product yield (% mole)			Product selectivity (% mole)			Total product selectivity (% mole)
		Fructose	Mannose	5-HMF	Fructose	Mannose	5-HMF	
1	28.1	1.0	0.1	17.0	3.6	0.1	60.5	64.4
2	29.0	0.9	0	13.8	3.1	0	47.6	50.7
3	35.7	0.8	0	12.8	2.2	0	35.9	38.1
4	33.7	0.9	0	14.0	2.7	0	41.5	44.2

S2.6 Ammonia temperature programmed desorption (TPD)

50 mg of catalyst contained within a quartz tube was heated to 200 °C at a ramp rate of 1 °C min^{-1}. After 2 hours the catalyst was cooled to 100 °C and dosed with an excess of 0.02 vol% ammonia in helium. The ammonia was then desorbed from the catalysts by heating the material to 400°C at a ramp rate of 2 °C min^{-1}. To ensure the complete desorption of ammonia from the material, the temperature was then maintained at 400 °C. The amount of ammonia desorbed from the catalyst was measured using a mass spectrometer and quantified at m/z = 15 to avoid interference with desorbed water. The TPD profile, Figure S8, shows three peaks, suggesting the presence at least three distinct acid sites within the material. The first peak appears around 150 °C. A second larger peak appears at around 250 °C, with a third desorption above 350 °C. The total acidity of the material is calculated as 0.39 mmol g^{-1}.

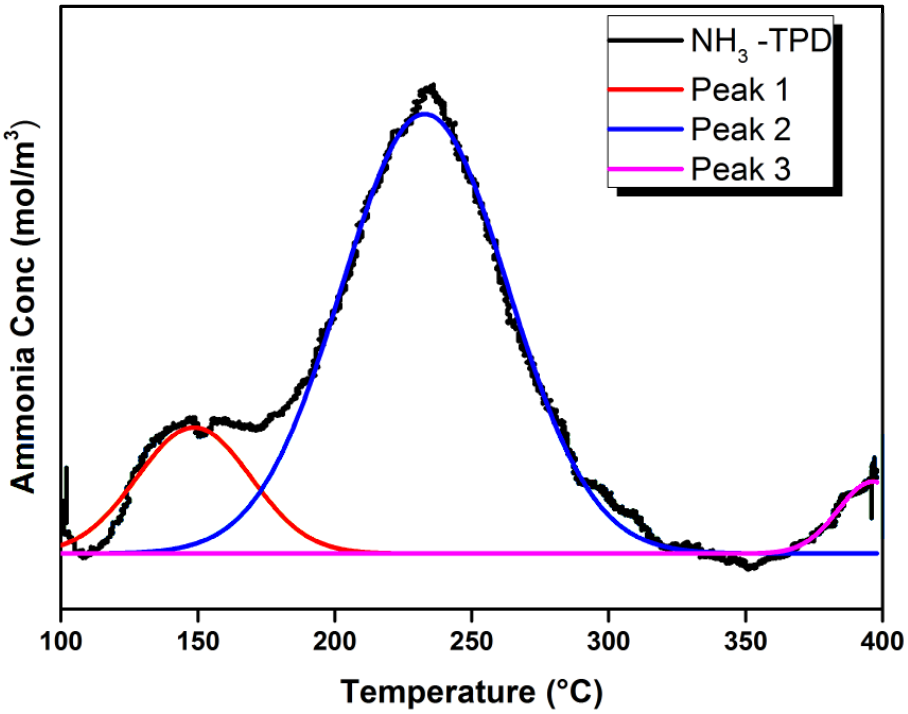

Figure S8: Ammonia TPD profile of (2).

Comparing these results with the literature on other solid-acid MOFs shows ammonia TPD occurs at similar temperatures. For example, Jiang *et al.* observed desorption of ammonia around 100 – 250 °C under similar condition for the Cu-containing MOF-74,[7] and in our previous work on MIL-88B(Fe,Sc) we observed desorption of ammonia from ~120 – 300 °C.[8]

2.7: Pyridine adsorption

Fourier transform infrared spectroscopy (FTIR) was performed using a Bruker ALPHA FT-IR spectrometer fitted with a diamond attenuated total reflection (ATR) stage. To measure the interaction with pyridine, two drops of liquid pyridine were added to small amount of powdered and freshly dried (200 °C) **(2)** *in situ* on the ATR stage. The excess pyridine was allowed to evaporate, as observed by the disappearance of its characteristic bands in the FTIR spectrum to reveal the bands of adsorbed pyridine. For comparison the spectrum of (2) alone was measured as shown in Figure S9.

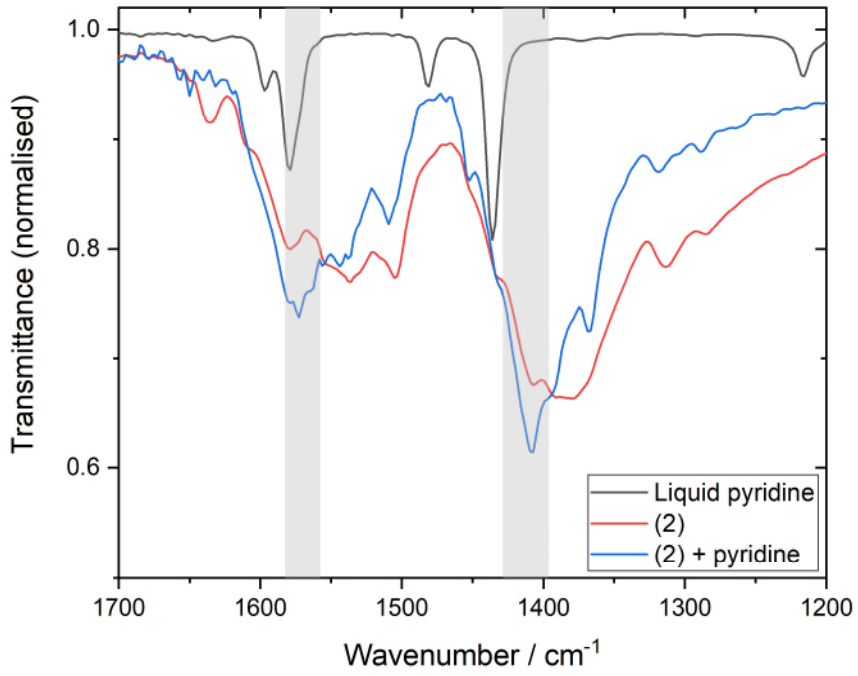

Figure S9: FTIR spectra measured during pyridine adsorption on (2) with bands due ot adsorbed pyridine highlighted in grey.

The bands of adsorbed pyridine are observed at 1572 cm^{-1} and 1407 cm^{-1}. There were assigned according to the literature: Bartzetti *et al.*, who studied a range of solid acids including zeolites,[9] showed that pyridinium interacting with Brønsted acid sites is responsible for an IR band at ~1400 cm^{-1}, while pyridine interaction with Lewis acid sites gives an IR band at 1576 cm^{-1}. This confirms the presence of both Brønsted and Lewis acid sites in **(2)**.

S3: Comparison of catalysis results with literature

Table S4: Reported optimum glucose conversion catalysis using zeolites and metal-organic frameworks where single-step conversions were studied.

Catalyst	Temp / Time	Solvent	Glucose Conversion	Product Yield	Selectivity	Reference	Notes
Zeolite Sn-beta	140 °C / 90 mins	Water	80 %	Not stated	30 % fructose	10	pH 1 needed for HMF to be detected (see next entry)
Zeolite Sn-beta + HCl	180 °C / 70 mins	H_2O/THF/NaCl	79 %	Not stated	72 % HMF	11	
MIL-101(Cr)-SO_3H	120 °C /2 hours	DMSO	Not stated	7 % 5-HMF	Not stated	12	Most of this paper reported conversion of fructose
MIL-101(Cr)-SO_3H	100 °C / 24 hours	Water	21.6 %	21.6 % fructose	100 % fructose	13	
MIL-101(Cr)-SO_3H	150 °C / 210 mins	Water: γ-valerolactone 1:9	100 %	44.9% 5-HMF	45.8% HMF	14	
MIL-101(Cr)-SO_3H	180 °C / 4 hours	water/THF/NaCl (1:2 vol/vol water:THF)	99.9%	80.7 % 5-HMF	80.7 % HMF	15	
MIL-101(Cr)-SO_3H	130 °C / 24 hours	water/THF 39:1	Not stated	29 % 5-HMF	Not stated	16	Yield reduced to 13−16% on re-use
NU-1000	140 °C/ 5 hours	water	60 %	2.3 % 5-HMF; 19 % fructose	3.8 % 5-HMF; 31.7 % fructose	17	NU-1000 is a Zr-containing MOF
PO_4-NU-1000	140 °C/ 5 hours	water:THF	97 %	25 % 5-HMF; 5 % fructose	25.8 5-HMF; 5.2 % fructose	17	Phosphate-modified NU-1000 MOF
UiO-66-SO_3H	140 °C / 3 hours	water	35.9 %	21.7 % fructose; 7.9 5-HMF	82.5 % fructose; 22.0 % 5-HMF	18	UiO-66 is a Zr-containing MOF.
MIL-88B(Fe,Sc)	140 °C / 3 hours	DMSO	70.7	3.3 % fructose; 1.4 % manose; 24.9 5- HMF	4.7 % fructose; 2.0 % manose; 35.3 % HMF	8	

S4: References

[1] M. I. Breeze, T. W. Chamberlain, G. J. Clarkson, R. P. de Camargo, Y. Wu, J. F. de Lima, F. Millange, O. A. Serra, D. O'Hare and R. I. Walton, *CrystEngComm* **2017**, *19*, 2424-2433.

[2] D. F. Weng, X. J. Zheng and L. P. Jin, *Eur. J. Inorg. Chem.*, **2006**, 4184

[3] A. C. Larson, R. B. V. Dreele, General Structure Analysis System (GSAS), Los Alamos National Laboratory Report 1994, LAUR 86-748.

[4] O.V. Dolomanov, L.J. Bourhis, R.J. Gildea, J.A.K. Howard, J.A.K. & H. Puschmann, *J. Appl. Cryst.*, **2009**, *42*, 339-341

[5] G.M Sheldrick, (2015). *Acta Crystallogr.* **2015**, *A71*, 3-8.

[6] G.M. Sheldrick, (2015). *Acta Crystallogr.*, **2015**, *C71*, 3-8.

[7] H.X. Jiang, J.L. Zhou, C.X. Wang, Y.H. Li, Y.F. Chen, M.H. Zhang, *Ind. Eng. Chem. Res.* **2017**, *56*, 3542-3550.

[8] R. Pertiwi, R. Oozeerally, D. L. Burnett, T. W. Chamberlain, N. Cherkasov, M. Walker, R. J. Kashtiban, Y. K. Krisnandi, V. Degirmenci and R. I. Walton, *Catalysts*, 2019, **9**, 437.

[9] T. Barzetti, E. Selli, D. Moscotti L. Forni, *J. Chem. Soc., Faraday Trans.*, 1996, **92**, 1401-1407.

[10] M. Moliner, Y. Roman-Leshkov and M. E. Davis, *Proc. Nat. Acad. Sci. USA*, 2010, **107**, 6164-6168.

[11] E. Nikolla, Y. Roman-Leshkov, M. Moliner and M. E. Davis, *ACS Catal.*, 2011, **1**, 408-410.

[12] J. Z. Chen, K. G. Li, L. M. Chen, R. L. Liu, X. Huang and D. Q. Ye, *Green Chem.*, 2014, **16**, 2490-2499.

[13] G. Akiyama, R. Matsuda, H. Sato, S. Kitagawa, *Chem. Asian J.* 2014, **9**, 2772–2777.

[14] Y. Su, G. G. Chang, Z. G. Zhang, H. B. Xing, B. G. Su, Q. W. Yang, Q. L. Ren, Y. W. Yang and Z. B. Bao, *AICHE J.*, 2016, **62**, 4403-4417.

[15] D. W. Chen, F. B. Liang, D. X. Feng, M. Xian, H. B. Zhang, H. Z. Liu and F. L. Du, *Chem. Eng. J.*, 2016, **300**, 177-184.

[16] A. Herbst and C. Janiak, *New J. Chem.*, 2016, **40**, 7958-7967.

[17] M. Yabushita, P. Li, T. Islamoglu, H. Kobayashi, A. Fukuoka, O. K. Farha and A. Katz, *Ind. Eng. Chem. Res.*, 2017, **56**, 7141-7148.

[18] R. Oozeerally, D. L. Burnett, T. W. Chamberlain, R. I. Walton and V. Degirmenci, *ChemCatChem*, 2018, **10**, 706-709.